Molecular Vision 2015; 21:1173-1184 <http://www.molvis.org/molvis/v21/1173>
Received 11 May 2015 | Accepted 11 October 2015 | Published 13 October 2015

Down-regulation of microRNA-155 attenuates retinal neovascularization via the PI3K/Akt pathway

Zhi Zhuang,[1] Xiao- qin,[2] He Hu,[1] Shi-yuan Tian,[2] Zhan-jun Lu,[2] Tian-zi Zhang,[2] Yu-ling Bai[2]

(The first two authors contributed equally to this manuscript.)

[1]Medical College, Inner Mongolia University for the Nationalities, Tongliao Inner Mongolia, China; [2]Department of Ophthalmology, Affiliated Hospital of Inner Mongolia University for the Nationalities, Tongliao Inner Mongolia, China

Purpose: We aimed to investigate the anti-angiogenic properties of miR-155 via in vitro and in vivo studies.
Methods: miR-155 was knocked down using lentivirus-mediated RNA interference. The proliferation, migration, and tube formation of human retinal microvascular endothelial cells (HRMECs) were measured using BrdU, Transwell, and Matrigel assays, respectively. An oxygen-induced retinopathy (OIR) model was induced using neonatal C57BL/6J pups. Anti-miR-155 was intravitreally injected on postnatal day 12, and the retinal non-perfused areas and extent of neovascularization were measured on postnatal day 18 using transcardiovascular fluorescein isothiocyanate (FITC)-dextran perfusion and retina sections. A laser-induced choroidal neovascularization (CNV) model was induced in adult C57BL/6J mice. To evaluate the leakage areas, fundus fluorescein angiography was performed on day 14 after anti-miR-155 intravitreal injection. The neovascularization area of the CNV model was also examined in confocal and retina section studies. The expression levels of SHIP1 and p-Akt (Thr308, Ser473, and Thr450) were evaluated both in vitro and in vivo.
Results: The expression of miR-155 was elevated in HRMECs after treatment with vascular endothelial growth factor (VEGF) and in neovascularized mouse model retinas. Anti-miR-155 lentivirus reduced the VEGF-induced proliferation, migration, and tube formation abilities of HRMECs. Anti-miR-155 attenuated retinal neovascularization in in vivo CNV and OIR models. In VEGF-treated HRMECs and retina neovascularization models, p-Akt (Ser473) was significantly upregulated, while SHIP1 was downregulated. Conversely, the inhibition of miR-155 restored the expression of SHIP1 and reduced the phosphorylation of effectors in the Akt (Ser473) signaling pathway.
Conclusions: The results revealed that the downregulation of miR-155 attenuated retinal neovascularization via the phosphatidylinositol 3-kinase (PI3K)/Akt pathway.

Retinal neovascularization is a major cause of vision loss in various diseases, such as retinopathy of prematurity (ROP), diabetic retinopathy (DR), and age-related macular degeneration (AMD), and the incidence rates of these diseases have recently increased [1]. Complications that result from uncontrolled retina neovascularization are the major causes of severe vision loss worldwide.

MicroRNAs (miRNAs, miR) are small (~20–22 nucleotides), non-coding RNAs that post-transcriptionally regulate gene expression by binding to the 3′-untranslated regions of target mRNAs, leading to mRNA degradation or the inhibition of translation [2]. miRNAs play a critical role in the regulation of diverse biologic processes, such as cell proliferation, differentiation, apoptosis, tissue development, and homeostasis [3-5]. Abnormal miRNA expression is associated with various human diseases, such as cancer and metabolic disorders [4].

miR-155 is a newly identified miRNA that has been associated with a large number of biologic activities, including lymphocyte activation, immune cell regulation, and microglia stimulation [6,7]. Accumulating studies have shown that miR-155 is upregulated in several diseases, such as breast cancer, colon cancers, Down syndrome, Alzheimer disease, multiple sclerosis, and even AMD [8-11]. Recently, miR-155 was reported to play an anti-angiogenic role in the regulation of neovascularization via the suppression of divergent cell-specific target genes [12]. Furthermore, several targets of miR-155, such as WEE1, SHIP1, and SOCS1, were identified in proteomic studies [13,14]. Moreover, functional studies have indicated that the phosphatidylinositol 3-kinase (PI3K)/Akt, c-JUN, and JAK/STAT pathways are constitutively activated by miR-155 overexpression [15,16]. Others also reported that inflammatory cytokines increase miR-155 expression in human retinal pigment epithelial cells (RPEs) [11], and in AMD miR-155 may be associated with inflammatory neurodegeneration [9]. However, the role of miR-155 in retinal angiogenesis remains unknown.

Correspondence to: Xiao-qin, Department of Ophthalmology, Affiliated Hospital of Inner Mongolia University for the Nationalities, Tongliao Inner Mongolia, China, 028000; Phone: 86-0475-8214451; FAX: 86-0475-8313345. email: dr_hanxiaoqin@163.com

In this study, we investigated the in vitro and in vivo anti-angiogenic effects of miR-155 using human primary retinal microvascular endothelial cells (HRMECs) and two kinds of mouse retinal neovascularization models. The results revealed that the downregulation of miR-155 attenuated retinal neovascularization via the PI3K/Akt pathway.

METHODS

Cells and animals: HRMECs (Angio-Proteomie, Boston, MA) are primary cells that were used for in vitro studies and were cultured as previously described [17]. Neonatal mice (C57BL/6J) and adult mice (C57BL/6J, 20~25 g) were purchased from the animal center of Inner Mongolia University and were raised in the animal room of the Affiliated Hospital of Inner Mongolia University for the Nationalities. This study adhered to the ARVO Statement for the Use of Animals in Ophthalmic and Vision Research and was performed in accordance with the guidelines provided by the Animal Care and Use Committee of the Affiliated Hospital of Inner Mongolia University for the Nationalities. The animals were housed with free access to laboratory food and water under a 12:12 h light:dark cycle.

Lentivirus transduction in HRMECs: HRMECs were transduced with anti-miR-155 (Thermo Scientific, MH12601, 5′-UUAAUGCUAAUCGUGAUAGGGGU-3′) or anti-control miRNA (Thermo Scientific, Anti-miR™ miRNA Inhibitor Negative Control #1, AM17010) in special endothelial growth medium (Endothelial Growth Medium, Cat# cAP-02, Angio-Proteomie, Boston, MA) for 24 h and cultured for another 24 h and 48 h in a medium that contained vascular endothelial growth factor ($VEGF_{165}$, 25 ng/ml, BD Biosciences, Cat#293-VE) as a stimulating factor. Anti-miR-155 or anti-miR GFP was applied with a lentivirus transduction agent (Thermo Scientific) following the guidelines provided by the manufacturer. The efficiency of the lentiviral particles that produced anti-miR-155 in the transduced cells was confirmed via fluorescence microscopy. Because HRMECs are primary endothelial cells, they are sensitive to nutritional deficiencies; thus, all of the culture media in our experiments contained 10% FBS (Life Science Technology, as suggested by the manufacturer's culture protocol), including media for the proliferation assay, migration assay, tube formation assay, and western blot studies.

Endothelial cell proliferation assays: The effects of anti-miR-155 on cell proliferation were studied using a BrdU Cell Proliferation Assay Kit (#6813, Cell Signaling Technology) as previously described [17]. Briefly, anti-miR-155-treated HRMECs were seeded at a density of 1×10^4 cells per well in 96-well plates and incubated for an additional 24 h and 48 h in a medium that contained $VEGF_{165}$. At the indicated time points, the proliferation assays were performed according to the manufacturer's instructions. Each experiment was performed in five wells and repeated at least three times.

Endothelial cell transwell migration assay: A transwell migration assay (Corning, Cat# 3422) was performed as previously described to evaluate the migration capacity of endothelial cells [17]. HRMECs were transduced with anti-ctrl or anti-miR155 lentivirus and cultured in VEGF-containing culture medium for 24 h. Afterwards, HRMECs were detached from the plate and re-suspended. Then, 2×10^4 cells from each group were placed in the top chamber in 200 µl of serum-free medium, and a volume of 600 µl of culture medium containing 10% FBS and VEGF was placed in the bottom chamber. During the transwell migration assay, 10% FBS-cultured HRMECs and VEGF-treated cells were used as controls. All migration assays were performed at 37 °C for 4 h. At the end of the assay, the cells were fixed in 4% PFA and stained with DAPI (Roche, Cat#10236276001) for 10 min. The cells that did not migrate were removed with a cotton swab, and the membrane was photographed. Cells from five random fields of view were counted.

Matrigel tube formation study: Two-hundred-microliter aliquots of Matrigel (BD Biosciences, Cat# 354,234) solution were poured into 48-well plates, and the plates were then incubated at 37 °C for 30 min in a 5% CO_2 incubator. Anti-miR-155-treated HRMECs (5×10^4 per well) were seeded on the Matrigel and cultured for another 12 h in a medium that contained $VEGF_{165}$. The networks in the Matrigel from five randomly selected fields were counted and photographed under a microscope. The experiments were performed in triplicate and repeated three times.

In situ hybridization: For in situ hybridization studies, 5 µm thick retinal paraffin-embedded sections were transferred to positively charged slides. An in situ hybridization (ISH) kit (Biochain Institute, Hayward, CA) was used to detect miR-155, with DIG-labeled custom-made mercury locked nucleic acid (LNA) miRNA detection probes (Exiqon, Vedbaek, Denmark). A scrambled probe was used as a control.

Induction of a mouse oxygen-induced retinopathy (OIR) model and assessment of angiography: On postnatal day 7 (P7), C57BL/6 pups were exposed to hyperoxia (75% oxygen) for five days. On P12, the animals were returned to room air to induce retinal neovascularization for five days. On P12, the OIR mice were intravitreally injected with 1 µl of anti-miR-155 (Thermo Scientific, MH19607, 5′-CUCCUACCUGUUAGCAUUAAC-3′) or a control agent (anti-ctrl; Thermo Scientific, Anti-miR™ miRNA Inhibitor Negative Control

#1, AM17010). On P18, the mice were perfused through the left ventricle with 0.5 ml of PBS that contained 50 mg of 2×10^6 molecular weight fluorescein-dextran-FITC (Sigma, St. Louis, MO). The retinas were viewed under a fluorescence microscope (Zeiss Axiophot, Thornwood, NY) and photographed. The non-perfused areas were analyzed with ImageJ software. The ratio of the non-perfused area to the entire retinal area was determined.

Induction of mouse choroidal neovascularization (CNV) models and assessment of angiography: CNV was induced in adult female C57BL/6J mice by laser photocoagulation (Coherent 130SL, Coherent, Santa Clara, CA) using the following settings: 532 nm, 150 mW, 100 ms, and 100 mm. Lesions were created in one eye, and the other eye was used as a control. After establishing the CNV model, 1 µl of anti-miR-155 or anti-ctrl was intravitreally injected into each eye. Fourteen days after laser photocoagulation, fluorescein angiography (FA) was performed using a digital imaging system (Phoenix Micron IV Retinal Imaging Microscope, Pleasanton, CA) according to the manufacturer's instructions. An intraperitoneal injection of 5% fluorescein was administered, and late-phase (5 min after injection) fundus angiograms were analyzed. The fluorescein leakage area for each lesion was measured using ImageJ software.

Measurement of CNV volume: Fourteen days after laser injury, eyes were enucleated and fixed with 4% paraformaldehyde (PFA). The eye cups were blocked for 30 min and then incubated overnight at 4 °C with 0.5% FITC-isolectin B4 (Vector Laboratories, Burlingame, CA). Then, the RPE-choroid-sclera complex was flatmounted in an antifade medium (Immu-Mount Vectashield Mounting Medium; Vector Laboratories). Flatmounts were examined with a confocal microscope (TCS SP; Leica, Heidelberg, Germany). Vessels were visualized at a wavelength of 488 nm, and the capture emission was between 515 to 545 nm. Horizontal optical sections (1 µm steps) were obtained from the surface of the RPE-choroid-sclera complex. The volume of CNV fluorescence was measured with software from the microscope manufacturer (TCS SP; Leica).

Quantitative assessment of retinal neovascularization in retina sections from the OIR and CNV models: Retinal neovascularization was evaluated using 6-µm paraffin-embedded sagittal sections from P18 mice (OIR model) or 14 days after laser CNV induction (CNV model) that were stained with hematoxylin and eosin (HE). In the OIR model, the nuclei of neovascularization extending beyond the inner limiting membrane (ILM) into the vitreous body were counted. For each eye, 10 sections were randomly chosen and evaluated, and sections that included the optic nerve were not used. In the CNV model, sagittal sections were cut through the center of the laser photocoagulation site. An average of four sections was used to evaluate the height of the CNV by measuring the B/C ratio, where B indicates the thickness between the bottom of the pigmented choroidal layer and the top of the neovascular membrane, and C indicates the thickness of the intact-pigmented choroid next to the lesion [18]. For each group, two researchers evaluated sections from six mice in a blinded protocol.

MicroRNA extraction and quantitative real-time PCR: Total RNA was isolated from HRMECs and mouse retinas using a TRIzol reagent (Invitrogen, CA), and its concentration and integrity were determined with UV spectrophotometry (NANODROP 2000C, Thermo Scientific). Levels of miR-155 were detected using a TaqMan microRNA Reverse Transcription Kit (Applied Biosystems). Briefly, 200 ng of total RNA from cells or retinas were used for primer-specific reverse transcriptase (RT) PCR for miR-155, and then 2 µl of the RT product was used for subsequent quantitative RT–PCR (qPCR). We calculated the changes in mRNA expression according to the $2^{-\Delta\Delta}$(cycle threshold) CT method, with $\Delta CT=C_{\text{Target gene}}-CT_{\text{ACTB}}$ and $\Delta\Delta CT=\Delta C_{\text{Treatment}}-\Delta CT_{\text{Control}}$.

The miR-155 primers for human samples were 5′-GCAGCTAGCCCAGGGTTGGAACTGAGTTTGA-3′ (forward primer) and 5′-GCAAAGCTTCAGTTAACCCG-GCGGTGA-3′ (reverse primer), and the primers for mouse samples were 5′-CTAGCTAGCGAACTATGAACCGTG-GCTG-3′ (forward primer) and 5′-CCGCTCGAGGAGAT-GTTGTTTAGGATACTGC-3′ (reverse primer). Each sample was measured in triplicate wells, and the experiments were repeated three times.

Western blot analysis: HRMECs and retina proteins were collected. NuPAGE Bis-Tris (10%) gels (Invitrogen) were used according to the manufacturer's instructions. The membranes were blocked with 10% fat-free milk and incubated with primary antibodies overnight at 4 °C. The primary antibodies were used at the following dilutions: anti-Akt (rabbit monoclonal, CST#9272, 1:1000), phospho-Akt (Thr308; rabbit monoclonal, CST#13038, 1:1000), phospho-Akt (Ser473; rabbit monoclonal, CST#4060, 1:1000), phospho-Akt (Thr450; rabbit monoclonal, CST#12178, 1:1000), and anti-SHIP1 (D1163; rabbit monoclonal, CST#2728, 1:1000). To control for lane loading, the same membranes were probed with anti-beta-actin (mouse monoclonal antibody, ab8226, 1:2000) after being washed with a stripping buffer. Relative changes in protein expression were calculated and expressed as fold changes. Each experiment was repeated at least three times.

Statistical evaluation: The data were analyzed using the following statistical software programs: Prism 5 (GraphPad Software Inc., San Diego, CA) and SPSS (SPSS, version 16.0; SPSS Science, Chicago, IL). All data are presented as mean ± SEM, and the normality of the distribution was assessed. Individual group means were compared using a Student's unpaired *t* test, and data sets were examined with a one-way ANOVA (ANOVA), followed by a post-hoc Dunnett's *t* test. A p value <0.05 was considered indicative of a significant difference.

RESULTS

Expression of miR-155 in HRMECs and mouse retinas after lentivirus transduction: Multiplicity of infection (MOI) values of 25, 50, and 100 were used to evaluate the transduction rate of miR-155 in HRMECs, and the results showed that an MOI of 50 effectively transduced HRMECs, with a transduction efficacy of over 90% (Supplemental Figure 1). Thus, this concentration was used for further studies.

As shown in Figure 1, VEGF-induced miR-155 expression in HRMECs (Figure 1A; p<0.0001 versus the 10% FBS cultured control group) and anti-miR-155 treatment significantly decreased the mRNA levels of miR-155 compared with the control group (Figure 1C; p<0.01 versus the untreated

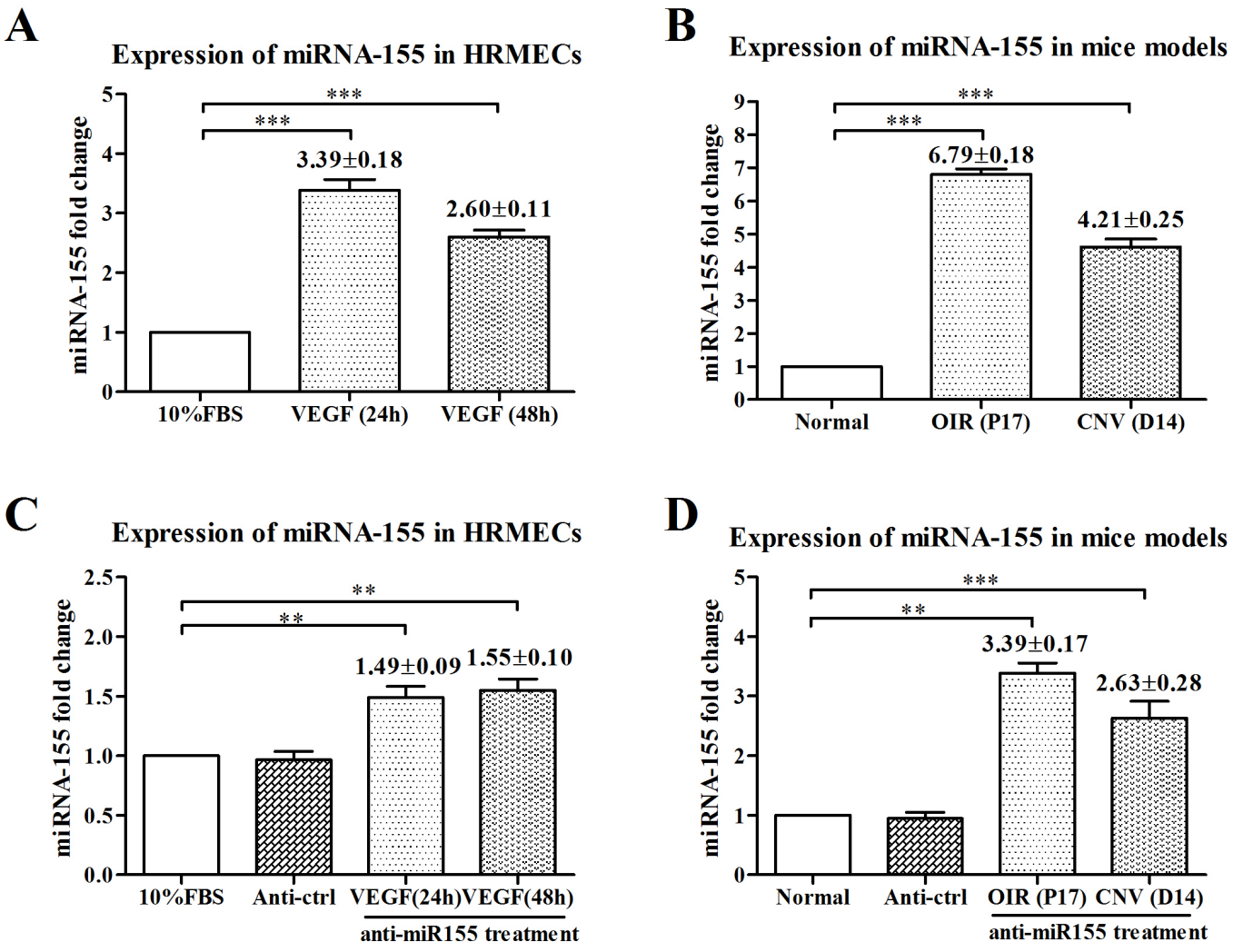

Figure 1. miR-155 expression in HRMECs under VEGF stimulation and mouse retina neovascularization. miR-155 was significantly upregulated in HRMECs at 24 h and 48 h after treatment with VEGF (**A**) and in the OIR and CNV model mouse retinas (**B**) compared with the normal control group. Anti-miR155 treatment reduced the expression of miR-155 in both HUMECs (**C**) and mouse retinas (**D**) compared to the normal control group and anti-control lentivirus treatment group. All experiments were repeated at least three times. The data are presented as mean ± SEM. *p<0.05, **p<0.01; ***p<0.001.

control group). In the retinal neovascularization animal model, miR-155 was also upregulated in the OIR and CNV models (Figure 1B; p<0.0001 versus the normal retina control group), and miR-155 levels decreased in response to treatment with anti-miR-155 (Figure 1D). There was no significant difference between the untreated HRMECs and anti-control transduction group, nor between the normal retina and anti-control-treated retina (Figure 1C,D). The absolute concentrations of miR-155 in HRMECs and retinas are presented in Supplementary Figure 2.

Anti-miR-155 reduced VEGF-induced cell proliferation, migration and tube formation of HRMECs: Vascular endothelial cell proliferation and migration are important for angiogenesis. As indicated in Figure 2A, anti-miR-155 inhibited VEGF-induced proliferation of HRMECs at various time points throughout the study.

Migration ability was assessed with a transwell migration assay. As shown in Figure 2B, significantly fewer anti-miR-155-treated HRMECs crossed the membrane compared with the VEGF-treated cells (Figure 2B, right panel).

A matrigel assay was used to evaluate the anti-angiogenic effects of miR-155 in vitro. In the present study, anti-miR-155 impaired cell capacity to form a regular network (Figure 2C). The length of the angiogenesis network also significantly differed compared with the VEGF-treated HRMECs (Figure 2C, right panel).

The effects of anti-miR-155 on the OIR model: Anti-miR-155 has been shown to inhibit tumor growth [19]. We also verified that miR-155 was co-localized with retinal capillaries (Supplementary Figure 3). To determine the effects of anti-miR-155 on the OIR mouse model, this agent was intravitreally injected into the right eyes of the retinopathy and age-matched normal mice on P12. As shown in Figure 3, anti-miR-155 reduced the non-perfused area of the retina to 17.31±1.2% (n=6), which significantly differed from the 29.74±1.5% (n=6) area observed in the controls (Figure 3A,B, p<0.01 compared with the anti-ctrl treated group).

Retinal neovascularization, as represented by endothelial cell nuclei protruding into the vitreous cavity, was decreased in the anti-miR-155 treated mice (Figure 3C,D). As shown in Figure 3, the average number of neovascular nuclei was 34.65±5.34 in anti-ctrl treated mouse eyes (n=6) and 16.54±1.98 in anti-miR-155 treated eyes (n=6; Figure 3D). There was a significant difference between the anti-miR-155 treated group and the control (p<0.01, Figure 3D).

The effects of anti-miR-155 on laser-induced CNV lesions: CNV leakage in mice was assessed by fluorescein angiography (FA) 14 days after laser photocoagulation. The right eyes of the mice were intravitreally injected with 1.0 µl of anti-miR-155 after the induction of CNV. Fourteen days after the induction of CNV, hyperfluorescent leakage was observed at the lesion sites in the mice (Figure 4A). As shown in Figure 4A, anti-miR-155 reduced the leakage area to 33.9±5.4%, which significantly differed from the anti-ctrl controls (p<0.01).

FITC-isolectin B4 was used to stain the neovascularization area of the laser-induced CNV. Confocal assessment indicated that the volume of the CNV in the anti- miR-155-treated group was $26.94\pm2.66\times10^4$ μm^3, and that in the anti-ctrl treated group was $56.19\pm2.01\times10^4$ μm^3; there was a significant difference between the two groups (Figure 4C,D; p<0.01).

Histologic CNV sections indicated reduced neovascularization and proliferative membranes in the laser lesion of the anti-miR-155 treated group compared to the anti-ctrl treated group, as shown in Figure 4E,F. There was a significant difference between the anti-miR-155 treated group (B/C ratio of 1.96±0.18) and the anti-ctrl treated group (B/C ratio of 4.07±0.18; Figure 4E,F, p<0.01).

Anti-miR-155-regulated SHIP1 and phospho-Akt (Ser473) signaling pathways: SHIP1 has been demonstrated to be the target of miR-155 in large B cell lymphoma (DLBCL) [16]. To verify the signaling pathways associated with miR-155 in HRMECs and retinal neovascularization, we performed in vitro and in vivo experiments to detect the protein expression levels of SHIP1 and p-Akt [p-Akt (Thr308), p-Akt (Ser473), p-Akt (Thr450)]. The results showed that anti-miR-155 treatment inhibited the expression of p-Akt (Ser473; p<0.05; Figure 4A) and increased the expression of SHIP1 (Figure 4B) in HRMECs after treatment with VEGF compared with the controls. We also examined in vivo SHIP1 and p-Akt (Ser473) protein expression levels in the retinas of the OIR and CNV mice. Figures 4C,D show that retinal neovascularization upregulated the expression of p-Akt (Ser473) and suppressed that of SHIP1 (Figures 4C,D). Anti-miR-155 effectively reduced the expression of p-Akt (Ser473; Figure 4C) and upregulated that of SHIP1 (Figure 4D) compared with the control group. There was no change in p-Akt (Thr308) and p-Akt (Thr450) expression in the present study.

DISCUSSION

Previous studies have shown that hypoxia and VEGF induce the expression of miR-155 [20]. In the present study, we confirmed that (1) VEGF can also induce the expression of miR-155 in HRMECs (Figure 1); (2) anti-miR-155 inhibited HRMEC proliferation (Figure 2A), migration (Figure 2B), and tube formation (Figure 2C); (3) retinal neovascularization

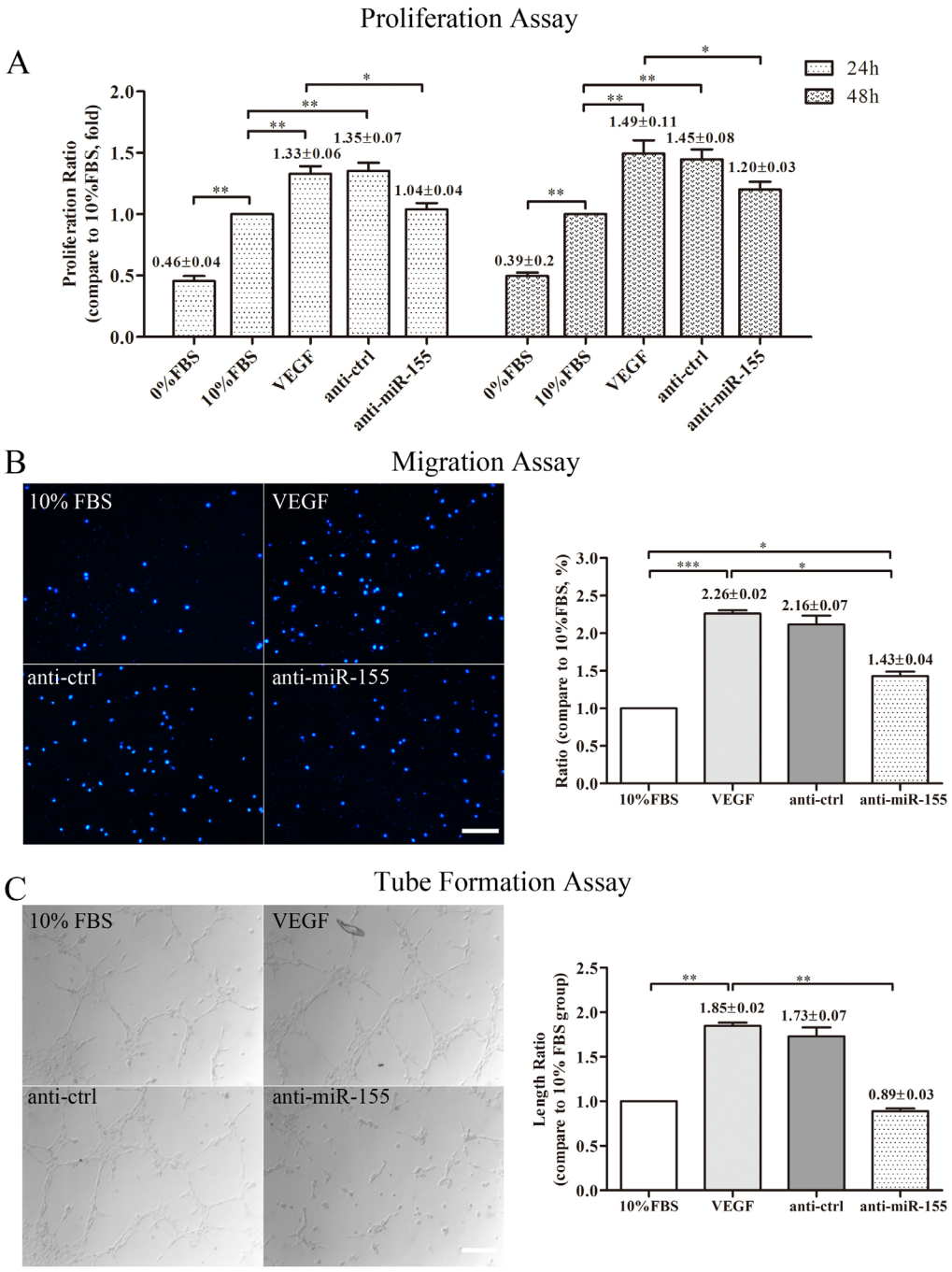

Figure 2. Effects of anti-miR-155 on VEGF-induced HRMEC proliferation, migration, and tube formation. VEGF-induced cell proliferation was inhibited in the anti-miR-155 treatment group at both 24 h and 48 h compared with the control groups (VEGF-treated control and anti-ctrl group; **A**). **B** shows representative images (10^{-6} mg/ml agents) of various treatment groups and the results of the statistical analysis. The cell nuclei were stained with DAPI, which is indicated in blue. Compared to the control group, the VEGF-induced migratory activities of the anti-miR-155 groups were inhibited (**B**). A Matrigel assay was used to evaluate tube formation. The total length of each tube in all treatment groups is presented. **C** shows the results of the statistical analysis and representative images of the various treatment groups. The tube formation study demonstrated that anti-miR-155 inhibited the effects of VEGF-induced angiogenesis. Each experiment was repeated at least three times. Data are presented as mean ± SD. *p<0.05, **p<0.01; ***p<0.0001. Scale bar: 20 µm.

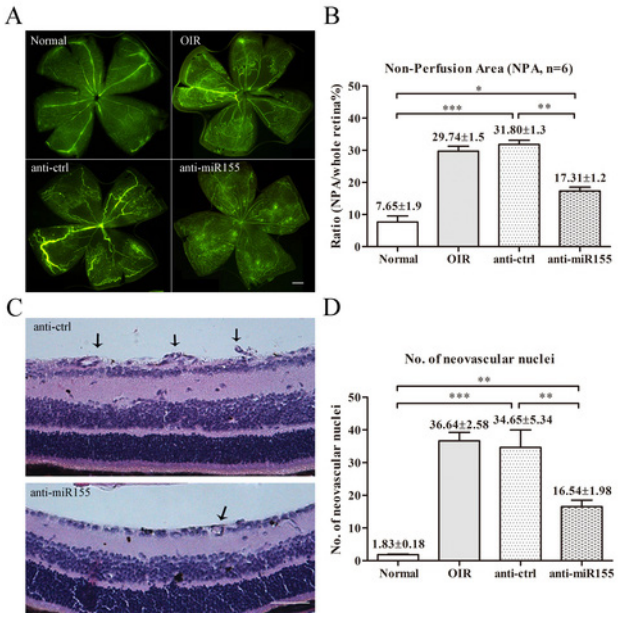

Figure 3. Effects of anti-miR-155 on retinal neovascularization in the OIR model. P7 mice were exposed to hyperoxia for five days. On P12, the pups were intravitreally injected with 1.5 µl of anti-miR-155. On P18, the pups were euthanized to detect the retinal non-vascularization areas and neovascular numbers. **A** and **B** show representative images of FITC-dextran-stained retinas from various treatment groups and the results of statistical analysis. **C** and **D** show representative mouse retina sections of the nuclei of neovascularization extending beyond the inner limiting membrane (ILM) into the vitreous body of the anti-ctrl and anti-miR-155 treated groups and the results of statistical analysis. The data are presented as mean ± SD. *p<0.05, **p<0.01, ***p<0.001. Scale bar: 50 µm.

animal models (OIR and CNV) expressed high rates of miR-155, and the inhibition of miR-155 reduced retinal neovascularization (Figure 3 and Figure 4); and (4) the inhibition of miR-155 restored the expression of SHIP1 and down-regulated the downstream PI3K-pAkt (Ser 473) signaling pathway in HRMECs and retinal neovascularization animal models (Figure 5).

Retinal neovascularization is described as the development of abnormal blood vessels within the retina [21]. Complications derived from retinal neovascularization, such as hemorrhage and retinal detachment, contribute to severe and irreversible visual loss in most patients [21]. Current knowledge indicates that neovascularization results from complex interactions between factors that either stimulate or inhibit endothelial cell differentiation, proliferation, migration, and maturation [1,22]. VEGF is the most important of these factors. To date, anti-VEGF therapy, such as ranibizumab and VEGF Trap-Eye, has yielded favorable clinical results for ROP, AMD, high myopia macular degeneration, and diabetic retinopathy [23]. However, the intravitreous injection of these anti-VEGF agents is associated with several problems, including the induction of retinal pigment epithelium tears, the accelerated proliferation of sub-retinal fibrosis, and the induction of macular atrophy. Therefore, exploring and evaluating the precise mechanisms of retinal neovascularization is important to identifying more effective therapeutic targets.

In recent years, various studies have demonstrated that miRNAs play a crucial role in oncogenesis, infection, and inflammation [2,5,9-11,14,24]. Because miRNAs are the key factors that post-transcriptionally regulate gene expression by controlling the translation and/or stability of target mRNAs, they influence many cellular activities under normal and disease conditions [4,6]. miR-155 is one of the most studied miRNAs and has been shown to be a typical multifunctional miRNA in various studies of various pathologies, including in tumors, Alzheimer disease, and AMD [9,14,25]. miR-155 is broadly expressed in different cell types, such as monocytes, macrophages, and dendritic cells [26,27]. There are also studies demonstrating its expression in human retinal pigment epithelial cells [11]. miR-155 has also been shown to act as an onco-miRNA in some situations, as it is upregulated and appears to be a key factor in the carcinogenesis of many cancers, such as lung cancer, colon cancer, B cell lymphoma, and chronic lymphocytic leukemia [4]. Currently, studies of the role of miR-155 in retina angiogenesis are rare. This study demonstrated that VEGF could upregulate the expression of miR-155 in retina-specific endothelial cells, which agrees

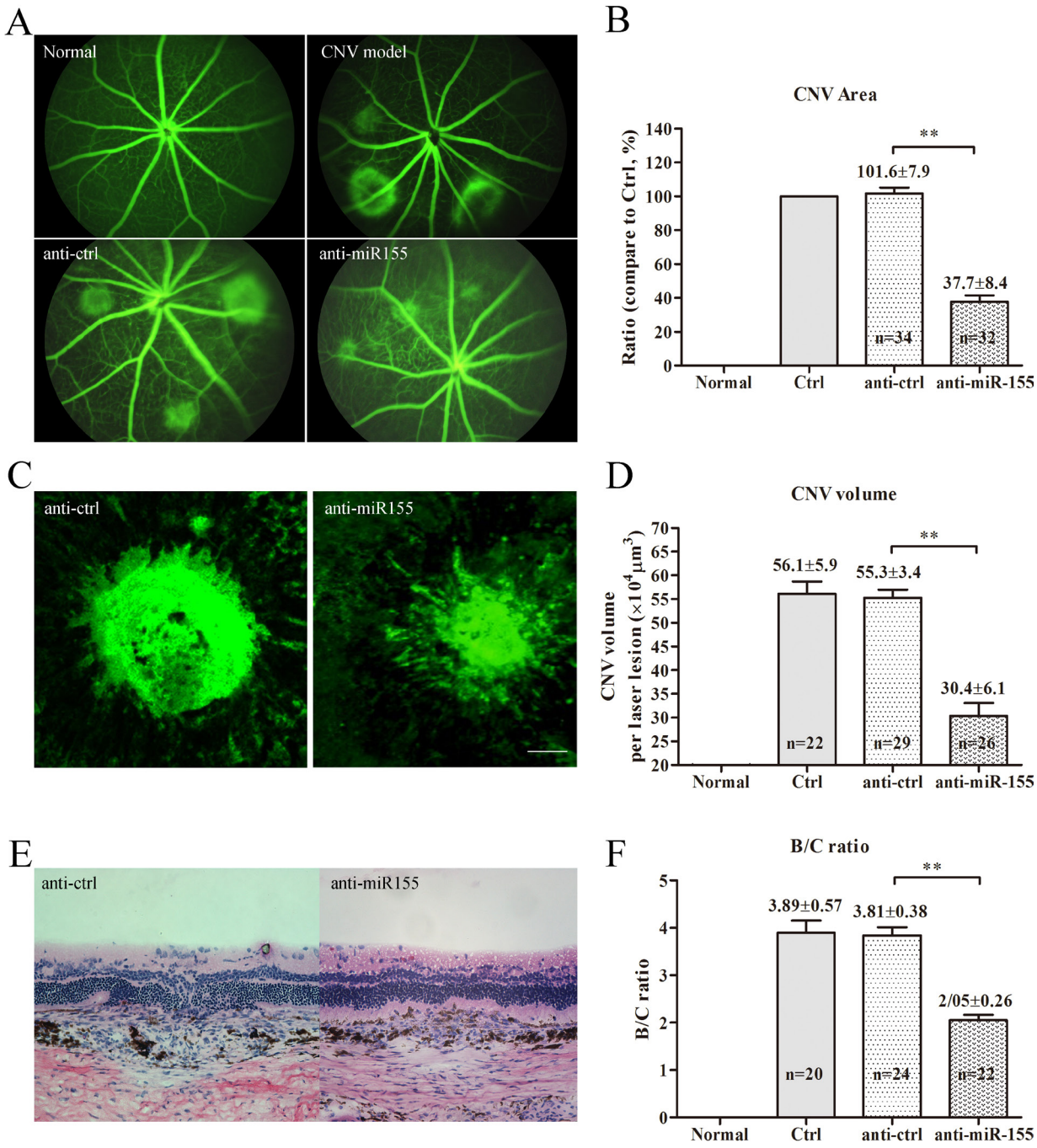

Figure 4. Effects of anti-miR-155 on retinal neovascularization in the laser-induced CNV model. Angiographic analysis of CNV leakage 14 days after laser photocoagulation in the various treatment groups and the control group. Panels **A** and **B** show representative images of retina FFA in various treatment groups and the results of statistical analysis. Panels **B** and **C** depict representative confocal images of the anti-ctrl and anti-miR-155 groups and the results of statistical analysis. Panels E and F are representative images of HE-stained sagittal sections of the anti-ctrl and anti-miR-155 groups and the results of statistical analysis. The data are presented as mean ± SD. *p<0.05, **p<0.01, ***p<0.001. Scale bar: 100 μm.

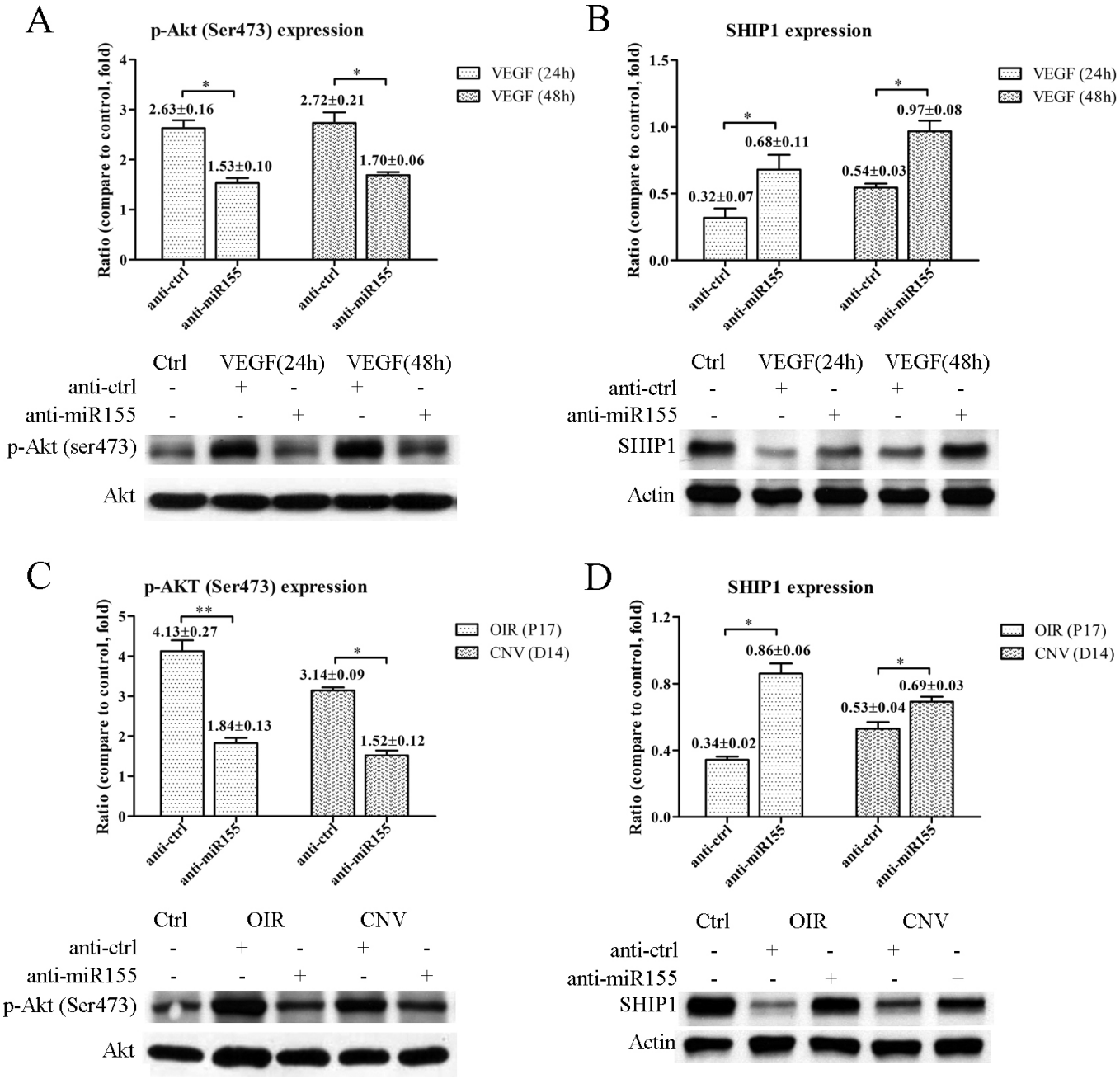

Figure 5. miR-155 activates the PI3K/Akt signaling pathway by targeting SHIP1**. A** and **B** show a schematic layout and the western blot results for the expression of p-Akt (Panel **A**) and SHIP1 (Panel **B**) in response to VEGF treatment with or without incubation with anti-miR-155. **C** and **D** show a schematic layout and western blot images of the expression of p-Akt (Ser473; Panel **C**) and SHIP1 (Panel **D**) after anti-miR-155 treatment in the OIR and CNV mouse models. Western blot results demonstrated that anti-miR-155 attenuated the expression of p-Akt (Ser473) and upregulated SHIP1 compared with the control group. All experiments were repeated at least three times. The data are presented as mean ± SEM. *p<0.05.

with the findings of a previous study by Kong and co-workers [20] that examined HUVECs. Moreover, miR-155 is also highly expressed in the OIR model (which resembles ROP patients) and the laser-induced CNV model (which resembles neo-vascular AMD patients). Furthermore, the inhibition of miR-155 significantly reduced retinal neovascularization. This evidence provides novel insight into present clinical therapy strategies; specifically, it identifies other pathways that downregulate VEGF signaling but do not influence the levels of VEGF itself. The results of this study indicate that miR-155 may be valuable for the development of pharmacology agents that combat anti-retinal neovascularization disease. Other studies have investigated the inflammatory role of miR-155 in neurodegenerative diseases and suggested that signaling pathways through NF-kB, JAT/STAT, and complement factor F may be important for the development and progression of these diseases [8,9,11]. Whether these pathways also affect the process of retina neovascularization in the context of the elevation of miR-155 still must be verified in future studies.

As stated previously, a proteomics study identified several targets of miR-155, including WEE1, SHIP1, and SOCS1, and miR-155 has been reported to repress the expression of SHIP1 [13,14]. SHIP1 is an inositol phosphatase that is known to convert the signaling molecule PIP3 to PIP2, whereas PI3K is responsible for the reverse reaction [28]. SHIP1 is well known to be a negative regulator of the kinase Akt, a downstream target of the PI3K pathway. The expression of endogenous SHIP1 in hematologic cells caused by the overexpression of miR-155 has been shown to increase Akt signaling [29]. This increase in Akt activity is secondary to the loss of SHIP1 and consequently the failure to hydrolyze PIP3, the active product of PI3K enzyme activity [30]. Furthermore, O'Connell and co-workers has shown that miR-155 represses SHIP1 via direct 3′UTR interactions that have been highly conserved throughout evolution [31]. miR-155 repressed endogenous SHIP1 following the sustained overexpression of miR-155 in hematopoietic cells, which increased the activation of kinase Akt [32]. However, the function of miR-155 on SHIP1 and PI3K/Akt has not been studied in neovascular retinal diseases. Similarly, this study also reported that high levels of miR-155 specifically reduced the levels of SHIP1, thereby promoting PI3K/Akt activation, in particular by inhibiting the expression of p-Akt (Ser 473). SHIP1 has also been suggested to be able to directly interact with the PI3K complex via an adaptor protein, which is a tyrosine-activated immunoreceptor [33]. In the present study, we identified and characterized a direct link between miR-155 and SHIP1, both in vivo and in vitro, whereby miR-155 can directly repress the expression of SHIP1 and activate p-Akt (Ser 473) signaling. Furthermore, we have also observed that the reciprocal effects of SHIP1 mirrored the decreasing levels of miR-155. Anti-miR-155 reduced the inhibition of SHIP1 and downregulated the activity of Akt. Thus, our studies indicated that the Akt signaling pathway directly participates in the regulation of miR-155 expression and SHIP1 levels in HRMECs and retinal tissue under neovascularization conditions.

In this study, we evaluated the anti-angiogenic activity of miR-155 both in vitro and in vivo. We confirmed that miR-155 significantly inhibited the proliferation, migration, and tube formation of HRMECs in vitro compared with controls. We used OIR and CNV animal models to evaluate the anti-angiogenic effects of miR-155 in vivo: anti-miR-155 significantly attenuated retina neovascularization in the laser-induced CNV and OIR models. The inhibition of miR-155 restored the expression of SHIP1 and facilitated the phosphorylation of effectors in the PI3K/Akt signaling pathway. Therefore, miR-155 plays a key role in the pathological programming of retinal neovascularization. However, further studies must be performed to verify in-depth mechanisms using miR-155 knockout mice, such as VEGF receptor signaling pathways.

APPENDIX 1. THE TRANSDUCTION EFFICACY OF MIR-155 IN HRMECS.

The left panel shows a representative fluorescence image of miR-155-transduced HRMECs cells, and the right panel shows a light microscopy picture of the same viewing field of transduced HRMECs. Scale bar: 100 µm. To access the data, click or select the words "Appendix 1."

APPENDIX 2. CONCENTRATIONS OF MIR-155 IN HRMECS AND RETINA.

The concentration in HRMECs is 144.8±29.6 fM, and the concentration in normal retina is 3150±489 fM. To access the data, click or select the words "Appendix 2."

APPENDIX 3. LOCALIZATION OF MIR-155 IN RETINA.

Panel A shows localization of miR-155 (blue chromogen) in the retinal capillaries (small arrow) and in the cells of inner nuclear layer (large arrow), probably in the retinal glial and neuronal cells. Panel B shows the scrambled control retina. To access the data, click or select the words "Appendix 3."

REFERENCES

1. Das A, McGuire PG. Retinal and choroidal angiogenesis: pathophysiology and strategies for inhibition. Prog Retin Eye Res 2003; 22:721-48. [PMID: 14575722].

2. Bartel DP. MicroRNAs: genomics, biogenesis, mechanism, and function. Cell 2004; 116:281-97. [PMID: 14744438].

3. Kloosterman WP, Plasterk RH. The diverse functions of microRNAs in animal development and disease. Dev Cell 2006; 11:441-50. [PMID: 17011485].

4. Calin GA, Croce CM. MicroRNA signatures in human cancers. Nat Rev Cancer 2006; 6:857-66. [PMID: 17060945].

5. Krutzfeldt J, Stoffel M. MicroRNAs: a new class of regulatory genes affecting metabolism. Cell Metab 2006; 4:9-12. [PMID: 16814728].

6. Thai TH, Calado DP, Casola S, Ansel KM, Xiao C, Xue Y, Murphy A, Frendewey D, Valenzuela D, Kutok JL, Schmidt-Supprian M, Rajewsky N, Yancopoulos G, Rao A, Rajewsky K. Regulation of the germinal center response by microRNA-155. Science 2007; 316:604-8. [PMID: 17463289].

7. Rodriguez A, Vigorito E, Clare S, Warren MV, Couttet P, Soond DR, van Dongen S, Grocock RJ, Das PP, Miska EA, Vetrie D, Okkenhaug K, Enright AJ, Dougan G, Turner M, Bradley A. Requirement of bic/microRNA-155 for normal immune function. Science 2007; 316:608-11. [PMID: 17463290].

8. Devier DJ, Lovera JF, Lukiw WJ. Increase in NF-kappaB-sensitive miRNA-146a and miRNA-155 in multiple sclerosis (MS) and pro-inflammatory neurodegeneration. Front Mol Neurosci. 2015; 8:5-[PMID: 25784854].

9. Lukiw WJ, Surjyadipta B, Dua P, Alexandrov PN. Common micro RNAs (miRNAs) target complement factor H (CFH) regulation in Alzheimer's disease (AD) and in age-related macular degeneration (AMD). Int J Biochem Mol Biol. 2012; 3:105-16. [PMID: 22509485].

10. Li YY, Alexandrov PN, Pogue AI, Zhao Y, Bhattacharjee S, Lukiw WJ. miRNA-155 upregulation and complement factor H deficits in Down's syndrome. Neuroreport 2012; 23:168-73. [PMID: 22182977].

11. Kutty RK, Nagineni CN, Samuel W, Vijayasarathy C, Hooks JJ, Redmond TM. Inflammatory cytokines regulate microRNA-155 expression in human retinal pigment epithelial cells by activating JAK/STAT pathway. Biochem Biophys Res Commun 2010; 402:390-5. [PMID: 20950585].

12. Pankratz F, Bemtgen X, Zeiser R, Leonhardt F, Kreuzaler S, Hilgendorf I, Smolka C, Helbing T, Hoefer I, Esser JS, Kustermann M, Moser M, Bode C, Grundmann S. MicroRNA-155 Exerts Cell-Specific Antiangiogenic but Proarteriogenic Effects During Adaptive Neovascularization. Circulation 2015; 131:1575-89. [PMID: 25850724].

13. Pedersen IM, Otero D, Kao E, Miletic AV, Hother C, Ralfkiaer E, Rickert RC, Gronbaek K, David M. Onco-miR-155 targets SHIP1 to promote TNFalpha-dependent growth of B cell lymphomas. EMBO Mol Med. 2009; 1:288-95. [PMID: 19890474].

14. Guedes JR, Custodia CM, Silva RJ, de Almeida LP, Pedroso de Lima MC, Cardoso AL. Early miR-155 upregulation contributes to neuroinflammation in Alzheimer's disease triple transgenic mouse model. Hum Mol Genet 2014; 23:6286-301. [PMID: 24990149].

15. McCoy CE, Sheedy FJ, Qualls JE, Doyle SL, Quinn SR, Murray PJ, O'Neill LA. IL-10 inhibits miR-155 induction by toll-like receptors. J Biol Chem 2010; 285:20492-8. [PMID: 20435894].

16. Huang X, Shen Y, Liu M, Bi C, Jiang C, Iqbal J, McKeithan TW, Chan WC, Ding SJ, Fu K. Quantitative proteomics reveals that miR-155 regulates the PI3K-AKT pathway in diffuse large B-cell lymphoma. Am J Pathol 2012; 181:26-33. [PMID: 22609116].

17. Bai Y, Zhao M, Zhang C, Li S, Qi Y, Wang B, Huang L, Li X. Anti-angiogenic effects of a mutant endostatin: a new prospect for treating retinal and choroidal neovascularization. PLoS ONE 2014; 9:e112448-[PMID: 25380141].

18. Sun Y, Yu W, Huang L, Hou J, Gong P, Zheng Y, Zhao M, Zhou P, Li X. Is asthma related to choroidal neovascularization? PLoS ONE 2012; 7:e35415-[PMID: 22567103].

19. Eis PS, Tam W, Sun L, Chadburn A, Li Z, Gomez MF, Lund E, Dahlberg JE. Accumulation of miR-155 and BIC RNA in human B cell lymphomas. Proc Natl Acad Sci USA 2005; 102:3627-32. [PMID: 15738415].

20. Kong W, He L, Richards EJ, Challa S, Xu CX, Permuth-Wey J, Lancaster JM, Coppola D, Sellers TA, Djeu JY, Cheng JQ. Upregulation of miRNA-155 promotes tumour angiogenesis by targeting VHL and is associated with poor prognosis and triple-negative breast cancer. Oncogene 2014; 33:679-89. [PMID: 23353819].

21. Zhang SX, Ma JX. Ocular neovascularization: Implication of endogenous angiogenic inhibitors and potential therapy. Prog Retin Eye Res 2007; 26:1-37. [PMID: 17074526].

22. Novack GD. Pharmacotherapy for the treatment of choroidal neovascularization due to age-related macular degeneration. Annu Rev Pharmacol Toxicol 2008; 48:61-78. [PMID: 17914929].

23. Fulton AB, Hansen RM, Moskowitz A, Akula JD. The neurovascular retina in retinopathy of prematurity. Prog Retin Eye Res 2009; 28:452-82. [PMID: 19563909].

24. Stanczyk J, Pedrioli DM, Brentano F, Sanchez-Pernaute O, Kolling C, Gay RE, Detmar M, Gay S, Kyburz D. Altered expression of MicroRNA in synovial fibroblasts and synovial tissue in rheumatoid arthritis. Arthritis Rheum 2008; 58:1001-9. [PMID: 18383392].

25. Wang YZ, Feng XG, Shi QG, Hao YL, Yang Y, Zhang AM, Kong QX. Silencing of miR155 promotes the production of inflammatory mediators in Guillain-Barre syndrome in vitro. Inflammation 2013; 36:337-45. [PMID: 23065188].

26. O'Connell RM, Rao DS, Chaudhuri AA, Boldin MP, Taganov KD, Nicoll J, Paquette RL, Baltimore D. Sustained expression of microRNA-155 in hematopoietic stem cells causes a myeloproliferative disorder. J Exp Med 2008; 205:585-94. [PMID: 18299402].

27. O'Connell RM, Rao DS, Chaudhuri AA, Baltimore D. Physiological and pathological roles for microRNAs in the

immune system. Nat Rev Immunol 2010; 10:111-22. [PMID: 20098459].

28. Backers K, Blero D, Paternotte N, Zhang J, Erneux C. The termination of PI3K signalling by SHIP1 and SHIP2 inositol 5-phosphatases. Adv Enzyme Regul 2003; 43:15-28. [PMID: 12791379].

29. Yamanaka Y, Tagawa H, Takahashi N, Watanabe A, Guo YM, Iwamoto K, Yamashita J, Saitoh H, Kameoka Y, Shimizu N, Ichinohasama R, Sawada K. Aberrant overexpression of microRNAs activate AKT signaling via down-regulation of tumor suppressors in natural killer-cell lymphoma/leukemia. Blood 2009; 114:3265-75. [PMID: 19641183].

30. Ooms LM, Horan KA, Rahman P, Seaton G, Gurung R, Kethesparan DS, Mitchell CA. The role of the inositol polyphosphate 5-phosphatases in cellular function and human disease. Biochem J 2009; 419:29-49. [PMID: 19272022].

31. O'Connell RM, Chaudhuri AA, Rao DS, Baltimore D. Inositol phosphatase SHIP1 is a primary target of miR-155. Proc Natl Acad Sci USA 2009; 106:7113-8. [PMID: 19359473].

32. Bhattacharyya S, Balakathiresan NS, Dalgard C, Gutti U, Armistead D, Jozwik C, Srivastava M, Pollard HB, Biswas R. Elevated miR-155 promotes inflammation in cystic fibrosis by driving hyperexpression of interleukin-8. J Biol Chem 2011; 286:11604-15. [PMID: 21282106].

33. Peng Q, Malhotra S, Torchia JA, Kerr WG, Coggeshall KM, Humphrey MB. TREM2- and DAP12-dependent activation of PI3K requires DAP10 and is inhibited by SHIP1. Sci Signal 2010; 3:ra38-[PMID: 20484116].

Articles are provided courtesy of Emory University and the Zhongshan Ophthalmic Center, Sun Yat-sen University, P.R. China. The print version of this article was created on 13 October 2015. This reflects all typographical corrections and errata to the article through that date. Details of any changes may be found in the online version of the article.